The RNG Turbulence Closure: Application and Revisited Performance Assessment

ALMERINDO D. FERREIRA[1] and ANTONIO C.M. SOUSA[2]
[1]Department of Mechanical Engineering, University of Coimbra,
Polo II, 3030 COIMBRA, PORTUGAL
[2]Department of Mechanical Engineering, University of New Brunswick,
P.O. Box 4400, Fredericton, NB, CANADA, E3B 5A3

Abstract: Despite the advances in high-performance computing, the use of sophisticated turbulence models, as for example LES, or direct numerical simulation (DNS), is not yet practicable in wind engineering problems. Due to the large areas usually studied, frequently two-equation closures are adopted for the simulation of the turbulence, due to their low computational requirements. In this paper, four two-equation turbulence models are tested for three cases of turbulent flow around isolated bluff bodies. The *RNG* model is revisited and its results are compared against the results produced by other eddy viscosity models (*MMK*, *k-w* and standard *k-ε*). Beyond some controversy on its derivation, the *RNG* model shows some advantage on the prediction of flows where separation, reattachment, and strong curvature phenomena are observed.

Keywords: Numerical simulation, bluff bodies, turbulence modelling, RNG turbulence model, shear flow, flow around buildings; two-equation turbulence model

1 Introduction

Many engineering applications require fluid dynamics studies to support different design stages. Often, wind tunnels are used to perform this task, however, with increasing frequency, computational fluid dynamics (CFD) is playing a very important role on this type of studies.

Wind engineering projects commonly deal with considerably large spaces, namely wind flows around several buildings [1]. This basically involves the modelling of turbulent flow around three-dimensional bluff bodies, a situation, which represents a constant challenge to fluid dynamicists due to its high complexity. In fact, the flow field generated includes several features such as strong streamline curvature, recirculation zones, stagnation and detachment points or lines.

For its simulation, and notwithstanding the tremendous increase of computational performance over the past few years, the grid refinement required, e.g., by the direct numerical simulation (DNS) or by the large eddy simulation (LES), precluded their use. Therefore, for this type of studies, the turbulence models chosen are usually based on two-equation closures. Examples are the standard *k-ε* model [2], hereafter referred as *k-ε* model, the *k-w* model [3], or the Reynolds Stress Model (RSM), also known as "Second Moment Closure - SMC" [4], just to mention a few.

When simulating the flow around bluff bodies, however, the standard *k-ε* model evidences considerable pitfalls – it does not predict, for example, the separation on top or on the sides of an isolated cubic obstacle, a phenomenon observed in several experimental studies [5].

The *RNG k-ε* model [6], hereafter just mentioned as *RNG* model, is frequently pointed out as a turbulence model that gives better predictions comparatively to the standard *k-ε* model, specially when separation and reattachment, as well strong streamline curvature are present (e.g., [7,8,9]).

There is, however, some controversy about the derivation of the *RNG* model, as pointed out by several authors [10,11,12,13]. In this paper, the *RNG* model is revisited as a follow-up to previous work [9], and its results are compared against those obtained with different turbulence models for three cases of wind flow around isolated bluff bodies.

2 Case studies

Three configurations were considered to accomplish the purpose of this study. In the first one, a surface-mounted cube (Figure 1a) is subjected to a turbulent boundary flow was simulated, for two incidence angles (γ=0° and γ=45°, respectively). The experimental results obtained by Castro and Robins [14] were used for comparison.

The second configuration corresponds to a square

cross section cylinder placed at the mid-height of a channel. The experimental results are provided by [15]. Figure 1b) shows a schematic representation of the computational domain adopted for this study. Several numerical tests for different lengths of *DL1* and *DL2* were performed, and flow around the body was found to be independent of the inflow and outflow conditions for *DL1=5H* and *DL2=10H*, respectively. According to the experiments, DV1 is equal to DV2, and it was set to 3.4H.

For the third configuration is considered a two-dimensional rib, mounted on the bottom of a rectangular duct, which was experimentally and numerically studied by [16]. These authors compared their experimental results with the computational predictions obtained using the standard *k-ε* model and the non-linear *k-ε* model proposed in [17]. These results will be commented later on in this work. The value of *H* and the location of the rib were set according to the experimental parameters provided in [16].
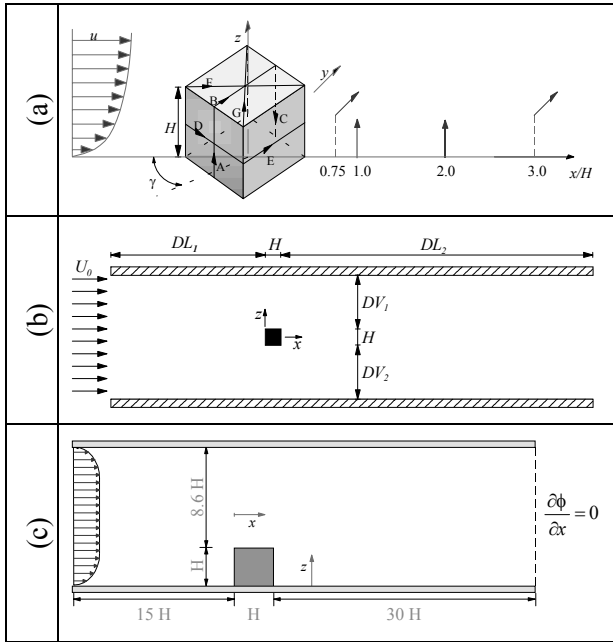

Fig. 1 - Schematic representation of the different configurations studied: (a) isolated cube; (b) square cylinder placed at the mid-height of the channel; (c) wall-mounted rib.

3 Numerical simulation methodology

3.1 Background
The wind flow for the different configurations was assumed to be governed by the three-dimensional (reduced to 2D for the last case, as mentioned before), incompressible, turbulent, steady-state equations of conservation of mass and momentum. These equations, continuity and Navier-Stokes equations, can be formulated as follows:

$$\frac{\partial u_i}{\partial x_i} = 0 \tag{1}$$

$$\frac{\partial}{\partial x_j}\left(\rho u_j u_i\right) = -\frac{\partial p}{\partial x_i} + \frac{\partial}{\partial x_j}\left[\mu\left(\frac{\partial u_i}{\partial x_j} + \frac{\partial u_j}{\partial x_i}\right) - \rho\overline{u_i' u_j'}\right] \tag{2}$$

The control volume formulation [18] was chosen for the discretization of the transport equations in a Cartesian coordinate system. Continuity and momentum equations are linked through pressure in accordance with the SIMPLEC formulation [19].

3.2 Turbulence models
The standard formulation of the *k-ε* model [3] was adopted as the base form for the evaluation of the Reynolds stress tensor. Using the eddy viscosity concept (μ_t) this model is expressed by the following equations:

$$\mu_t = C_\mu\frac{\rho k^2}{\varepsilon} \tag{3}$$

$$-\rho\overline{u_i' u_j'} = \mu_t\left(\frac{\partial u_i}{\partial x_j} + \frac{\partial u_j}{\partial x_i}\right) - \frac{2}{3}\delta_{ij}\rho k \tag{4}$$

$$\frac{\partial}{\partial x_j}\left(\rho u_j k\right) = \frac{\partial}{\partial x_j}\left[\left(\mu + \frac{\mu_t}{\sigma_k}\right)\frac{\partial k}{\partial x_j}\right] + P - \rho\varepsilon \tag{5}$$

$$\frac{\partial}{\partial x_j}\left(\rho u_j \varepsilon\right) = \frac{\partial}{\partial x_j}\left[\left(\mu + \frac{\mu_t}{\sigma_\varepsilon}\right)\frac{\partial\varepsilon}{\partial x_j}\right] + C_{\varepsilon 1}\frac{\varepsilon}{k}P$$
$$- C_{\varepsilon 2}\rho\frac{\varepsilon^2}{k} \tag{6}$$

where the production term *P* is expressed as

$$P = \mu_t\left(\frac{\partial u_i}{\partial x_j} + \frac{\partial u_j}{\partial x_i}\right)\frac{\partial u_i}{\partial x_j} \tag{7}$$

In Eqs. 1-7, u_i stands for the mean velocity component in the x_i direction (tensorial notation), *p* the mean pressure, *ρ* the density, *ε* the dissipation rate of turbulence energy, *k* the turbulent energy given by $k = \overline{u_i' u_i'}/2$, *μ* and μ_t the molecular and eddy viscosity respectively. For the *MMK* model [20], the C_μ constant in Eq. (3) is replaced by C_μ^*, which is a function of S and Ω, the mean strain rate and vorticity, respectively:

$$C_\mu^* = C_\mu\frac{\Omega}{S} \qquad \left(\frac{\Omega}{S} < 1\right) \tag{8a}$$

$$C_\mu^* = C_\mu \qquad\qquad \left(\frac{\Omega}{S} \geq 1\right) \qquad (8b)$$

For the *RNG* derivation, Yakhot et al. [6], using the renormalization group theory, determined all the model constants, and suggested the inclusion of an extra term in the right-hand side of the dissipation transport, Eq. (6) of the *k-ε* standard model. This term (*R*) "is of the same order of magnitude as the standard ε-production term in flow regions of large strain rate", as noted in [7], and is formulated as:

$$R = -\frac{\rho C_\mu \eta^3 \left(1 - \eta/\eta_o\right)}{1 + \beta\eta^3} \frac{\varepsilon^2}{k} \qquad (9)$$

where: $\eta = Sk/\varepsilon$; $S^2 = 2S_{ij}S_{ij}$.
The *k-w* model, according with [3], with *P* given by Eq. (7), is expressed by the following equations:

$$\frac{\partial}{\partial x_j}\left(\rho u_j k\right) = \frac{\partial}{\partial x_j}\left[\left(\mu + \sigma^* \mu_t\right)\frac{\partial k}{\partial x_j}\right] + P - \beta^* \rho w k \quad (10)$$

$$\frac{\partial}{\partial x_j}\left(\rho u_j w\right) = \frac{\partial}{\partial x_j}\left[\left(\mu + \sigma \mu_t\right)\frac{\partial w}{\partial x_j}\right]$$
$$+ \alpha\frac{w}{k}P - \beta\rho w^2 \qquad (11)$$

The constants for the different models used in this study are listed in Table 1.

Table 1. Turbulence model constants values

Model	Cμ	$C_{\varepsilon 1}$	$C_{\varepsilon 2}$	σ_k	σ_ε	η_0	β
k-ε *MMK*	0.09	1.45	1.9	1.0	1.3	--	--
RNG	0.085	1.42	1.68	0.72	0.72	4.38	0.015
k-w	α	β	β*	σ	σ*		
	5/9	3/40	0.09	0.5	0.5		

3.3 Boundary conditions
Inlet conditions for the different cases were set as those of the respective experiments. For the first case, the velocity profile at the entrance is given by a power law [14]. The inlet values for *k* and *ε* were imposed as in [5], as they studied the same case with an approximately equal incident velocity profile. For the second case, a uniform profile was assumed and the value of the U_0 was set to achieve a Reynolds number of 22000, based on *H* and U_0. The experimental value of 6% for the turbulence intensity was used to set the turbulent kinetic energy

at the entrance, and the dissipation rate was imposed using the procedure suggested in [21]. Finally, for the third case, the inlet conditions for *u, k* and *ε* use the values provided in [16].
The boundary conditions near the solid walls were implemented using wall functions as presented in [21]. At the outlet, in addition to the global conservation of mass, all variables were assumed to have a zero-gradient normal to the computational outflow area.

4 Results

4.1 Surface-mounted cube
The experimental values provided in [14] for the non-dimensional surface pressure coefficient ($Cp = (p-p_0)/(1/2\rho U_0^2)$, where the index "$_0$" refers to the undisturbed flow conditions, along the different lines A to G (Fig. 1a), as well longitudinal and transverse velocity profiles at several locations.

Figure 2a) shows, as a typical result, the surface pressure distribution along line E, for γ=0º and it can be observed that the *k-w* model presents the largest discrepancies. All other models predict reasonably well the pressure distributions along that line, with *RNG* showing a slight improvement over the *MMK* model. Similar conclusion can be drawn for the vertical profile of the longitudinal-velocity component presented in Figure 2b).

Notwithstanding the good agreement just mentioned, none of the tested models was able to predict the recirculation zone at the top of the cube, which was experimentally observed in [14]. Nevertheless, along the lateral surfaces, also for γ=0º, both *RNG* and *MMK* models predict a recirculation zone at the level *z/H*=0.5, as indicated by the experimental observations [5]. The *k-ε* model just predicts this recirculation zone at lower levels, as shown in the streamline diagrams (Figs. 3a and 3b).
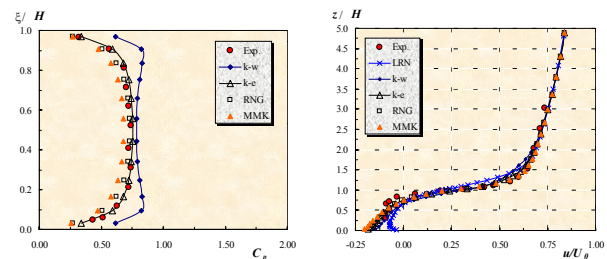

Fig. 2 - Pressure distribution along line E (Fig. 1a) [left]; and vertical profile of *u* on top of the cube at (*x*=0, *y*=0) [right], for γ=0º.

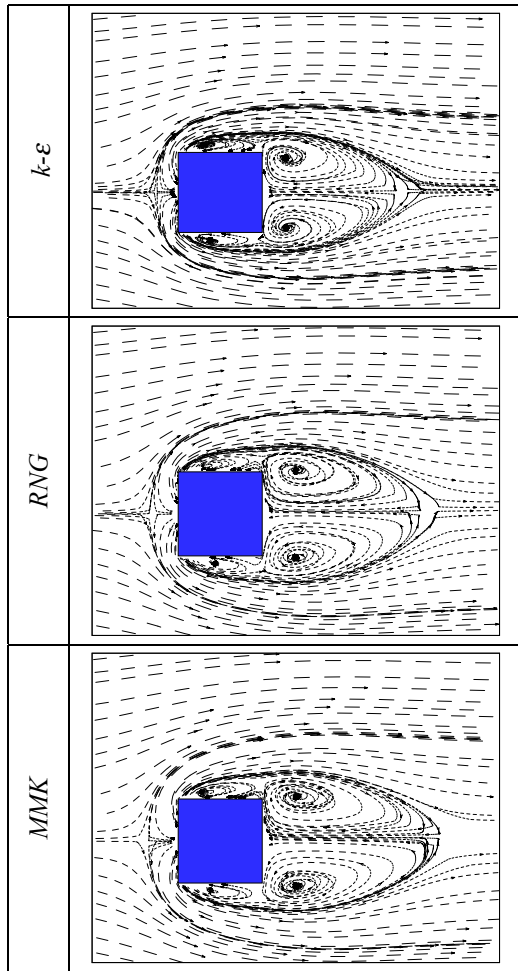Fig. 3a – Velocity streamlines at plane *z/H*=0.06 for the flow around an isolated cube (γ=0º).
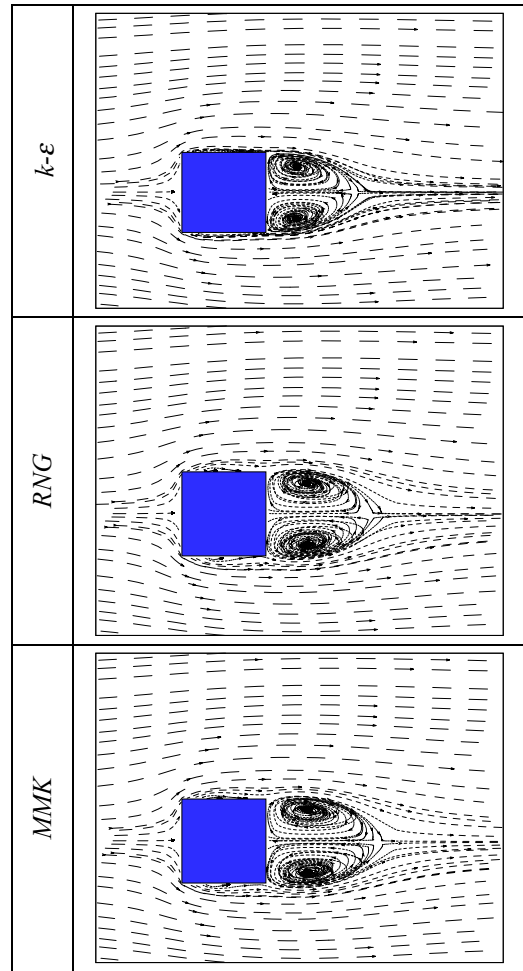

Fig. 3b – Velocity streamlines at plane *z/H*=0.5 for the flow around an isolated cube (γ=0º).

4.2 Flow around a cross-section cylinder

Concerning the second configuration studied, Fig. 4 presents a compilation of the results from different studies, and shows the streamwise variation of the longitudinal mean velocity component. Succinctly, it can be said that even the more elaborated turbulence models show some considerable discrepancies in the backward region of the cylinder, like the results obtained in the present work with *k-ε*, *RNG*, *k-w* and also with a low-Reynolds *k-ε* model (LRN).

The two diagrams in Fig. 5 display the vertical variation of *u*. The *RNG* model is, despite the apparent discrepancies, the only one predicting a recirculation zone - negative values of *u* - above the obstacle, as shown at two different locations (*x/H*=0.25 and *x/H*=0.75). The *k-w* model, for this particular case, presents the poorest performance.
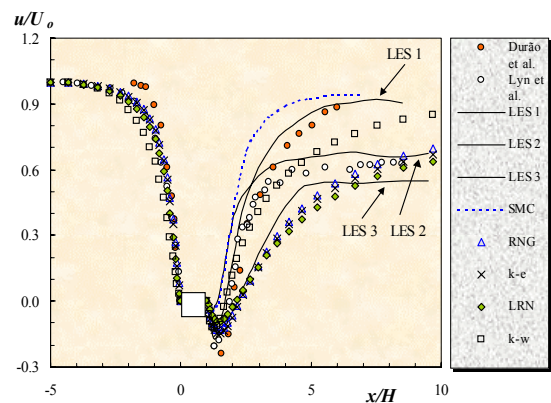

Fig. 4 - Streamwise variation of the longitudinal velocity component along the line *z*=0 for the second study case. LES [22]); SMC [23].
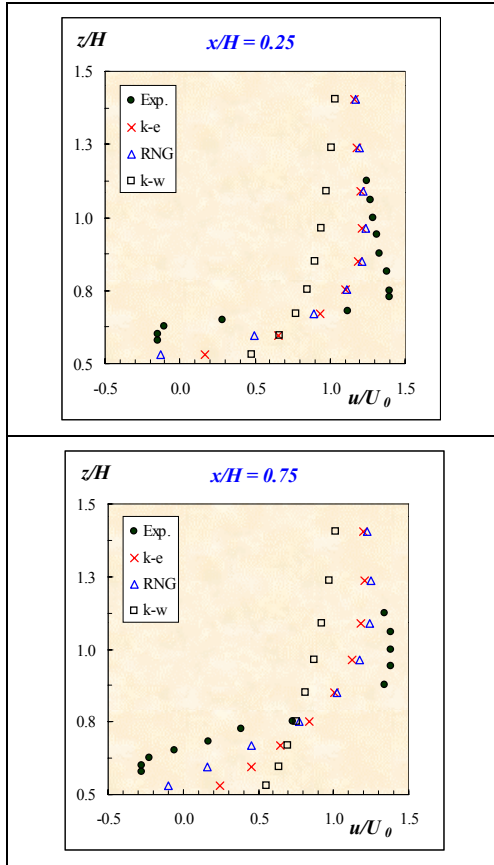
Fig. 5 - Experimental and numerical distributions of the longitudinal velocity component for the second configuration.
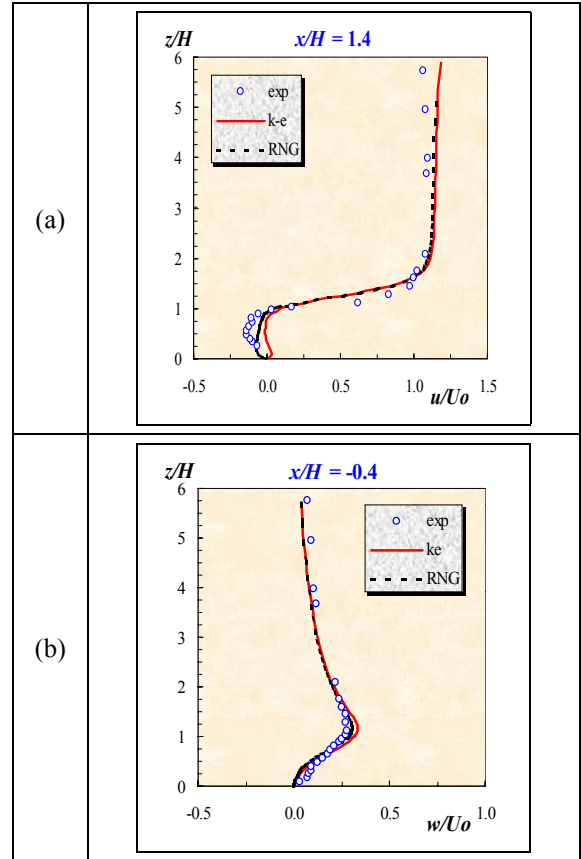

Fig. 6 - Comparison between experimental [16] and numerical results for: (a) the longitudinal (*x/H*=1.4), and (b) vertical (*x/H*=-0.4) velocity components for the third configuration.

4.3 Surface-mounted rib at the bottom wall of a rectangular duct

The two diagrams in Fig. 6 show the distribution of the longitudinal and the vertical velocity components, respectively, at two different locations. Just the *RNG* and *k-ε* models were employed in this study. Figure 6, and in particular Fig. 6a, clearly indicates that the *RNG* model has superior predictability as compared to that of the *k-ε* for the recirculation zone, i.e., for *z/H* smaller than 1.

In terms of the reattachment length (x_R/H), Table 2 compiles the present results against those presented at [16]. From this comparison, *RNG* shows the closest value comparatively to the experiments, even better than the obtained with the nonlinear *k-ε* model (n/ln) [17], which requires considerably larger CPU time than that for the *RNG*.

Table 2: Reattachment location (x_R) downstream of the wall-mounted rib

	Present results		Acharya *et al.*[16]		
	k-ε	*RNG*	Exp.	*k-ε*	n/ln*
X_R/H	6.8	7.5	7.3 ± 0.9	6.9	8.5

5 Conclusion

Three physical configurations (cube, and square cylinder placed at the half height of a channel, and a surface-mounted rib on a wall of a rectangular duct) were adopted for performance tests of several turbulence models (standard *k-ε*, *RNG*, *MMK*, and *k-w*). The different cases studied indicate that the *RNG* model produces similar results to the *MMK* model, while the *k-ε* and *k-w* have lower performance, particularly in the recirculation zones.

In two of the cases, *RNG* and other more involved models have similar prediction capability, despite the considerable less CPU time and computer requirements needed by *RNG* model.

To conclude, and in corroboration with previous work [9], and without giving consideration to the derivation's issues criticised in some publications [12,13], the authors fully support the statement made by Smith and Woodruff [7] "(…) the *RNG* model is a step beyond the standard model". Moreover, the numerical tests conducted do reiterate that the *RNG* model provides sufficient accuracy for assessment and design stages, and it can be considered to be a

useful tool in many applications of the wind engineering field.

References:

[1] Ferreira, A.D., Sousa, A.C.M., Viegas, D.X., "Numerical and experimental simulation of the wind field in the EXPO '98 area", *Wind & Structures - An International Journal*, Vol. 1, No. 4, 1998, pp. 337-349.

[2] Launder, B.E., Spalding, D.B., "The numerical computation of turbulent flows", *Computer Methods in Applied Mechanics and Engineering*, Vol. 3, 1974, pp. 269-289.

[3] Wilcox, D.C., *Turbulence Modeling for CFD*, DCW Industries, Inc., La Canada, California, 1993, 460 pages.

[4] Launder, B.E., Reece, G.J., Rodi, W., "Progress in the development of a Reynolds stress turbulence closure", *J. Fluid Mechanics*, Vol.68, 1975, pp. 537-566.

[5] Murakami, S., Mochida, A., "Three-dimensional numerical simulation of turbulent flow around buildings using the k-ε turbulence model", *Building and Environment*, Vol.24, 1989, pp. 51-64.

[6] Yakhot, V., Orszag, S.A., Thangam, S., Gatski, T.B., Speziale, C.G., "Development of turbulence models for shear flows by a double expansion technique", *Physics of Fluids - A*, 4, 1992, pp. 1510-1520.

[7] Smith, L.M, S.L. Woodruff, "Renormalization-group analysis of turbulence", *Annual Review of Fluid Mechanics*, Vol.30, 1998, pp. 275-310.

[8] Yin, M., Shi, F., Xu, Z., "Renormalization group based k-ε turbulence model for flows in a duct with strong curvature", *Int. J. Engineering Science*, Vol. 34, No. 2, 1996, pp. 243-248.

[9] Ferreira, A.D., Sousa, A.C., Viegas, D.X., "Numerical tests of the k-ε and RNG turbulence models for the flow around a 3D surface mounted obstacle". *Proceedings 9th Annual Conference of the CFD Society of Canada*, Waterloo, Canada, 27-29 May 2001, Ed. G.E. Schneider, pp.524-529.

[10] Lam, S.H., "On the RNG theory of turbulence", *Physics of Fluids A*, Vol.4, 1992, pp. 1007-1017.

[11] Eyink, G., "The renormalization group method in statistical hydrodynamics", *Physics of Fluids A*, Vol. 6, 1994, pp. 3063-3078.

[12] Nagano, Y., Itazu, Y., "Renormalization group theory for turbulence: Assessment of the Yakhot-Orszag-Smith theory", *Fluid Dynamics Research*, Vol. 20, 1997, pp. 157-172.

[13] Nagano, Y., Itazu, Y., "Renormalization group theory for turbulence: eddy-viscosity type model based on an iterative averaging method", *Physics of Fluids*, Vol.9, No.1, 1997, pp.143-153.

[14] Castro, I.P., Robins, A.G., "The flow around a surface-mounted cube in uniform and turbulent streams", *J.Fluid Mech.*, Vol.79, 1977, 307-335.

[15] Durão, D.F.G., Heitor, M.V., Pereira, J.C.F., "Measurements of turbulent and periodic flows around a square cross-section cylinder", *Experiments in Fluids*, Vol. 6, 1988, 298-304.

[16] Acharya, S., Dutta, S., Myrum, T.A., Baker, R.S., "Turbulent flow past a surface-mounted two-dimensional rib", *J. Fluids Engineering*, Vol. 116, 1994, pp. 238-246.

[17] Speziale, C.G., "On nonlinear k-l and k-ε models of turbulence", *J. Fluid Mechanics*, Vol. 178, 1987, pp. 459-475.

[18] Patankar, S.V., *Numerical Heat Transfer and Fluid Flow*, Hemisphere Publishing Corporation, Washington, D.C., 1980, 197 pages.

[19] Van Doormaal, J.P., Raithby, G.D., "Enhancements of the SIMPLE method for predicting incompressible flow", *Numerical Heat Transfer*, Vol. 7, 1984, pp. 147-163.

[20] Tsuchiya, M., Murakami, S., Mochida, A., Kondo, K., Ishida, Y., "Development of a new k-ε model for flow and pressure fields around bluff body", *J Wind Engineering and Industrial Aerodynamics*, Vol. 67&68, 1997, pp. 169-182.

[21] Versteeg, H.K., Malalasekera, W., *An Introduction to Computational Fluid Dynamics: The Finite Volume Method*. New York: Wiley, 1995, 257 pages.

[22] Rodi, W., Ferziger, J.H., Breuer, M., Pourquié, M., "Status of large eddy simulation: results of a workshop", *J. Fluids Engineering*, Vol. 119, 1997, pp. 248-262.

[23] Franke, R., Rodi, W., "Calculation of vortex shedding past a square cylinder with various turbulence models", *Proceedings of 8th Symposium on Turbulent Shear Flows*, Berlin, 1993, pp. 189-204.